Electronic Supplementary Material (ESI) for Physical Chemistry Chemical Physics.

Electronic Supporting Information for:

Polaron-formation revealed by transient XUV imaginary refractive index changes in different iron compounds

Wenfan Chen[a], Wei Xiong[a,b]

a. Materials Science and Engineering Program, University of California, San Diego.

b. Department of Chemistry and Biochemistry, University of California, San Diego.

S1. Sample preparation

Akaganeite was prepared by depositing Fe_2O_3 on glass slides, using sputter deposition for 30 mins by Denton Discovery 18 Sputter System. Hematite was prepared by depositing Fe on glass slides by sputtering for 10 mins using Denton Discovery 18 Sputter System and annealing at 520℃ in air for 2h using Ceramic tube furnace.

S2. Sample characterization

S2.1 X-ray Photoelectron Spectroscopy

The XPS of both hematite and akageneite are measured by PHI Quantera Scanning XPS. The spectral fitting was done by the software CASAXPS. The peak at 706eV and 720eV correspond to the Fe^{3+} $2p_{3/2}$ and $2p_{1/2}$ transitions. The peak at 711eV and 727eV correspond to the satellite peaks of Fe^{3+}.

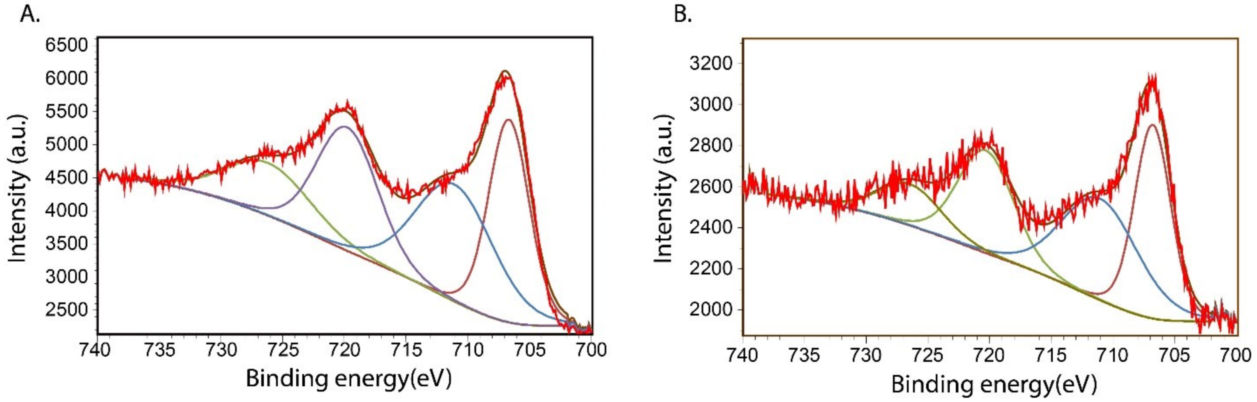

Figure S1. XPS of hematite(A) and akageneite(B) thin film.

S2.2 X-ray Diffraction

The XRD of both samples are measured by Bruker PXRD D8 advance X-ray diffractometer. The result indicates that the two samples are hematite and akageneite.

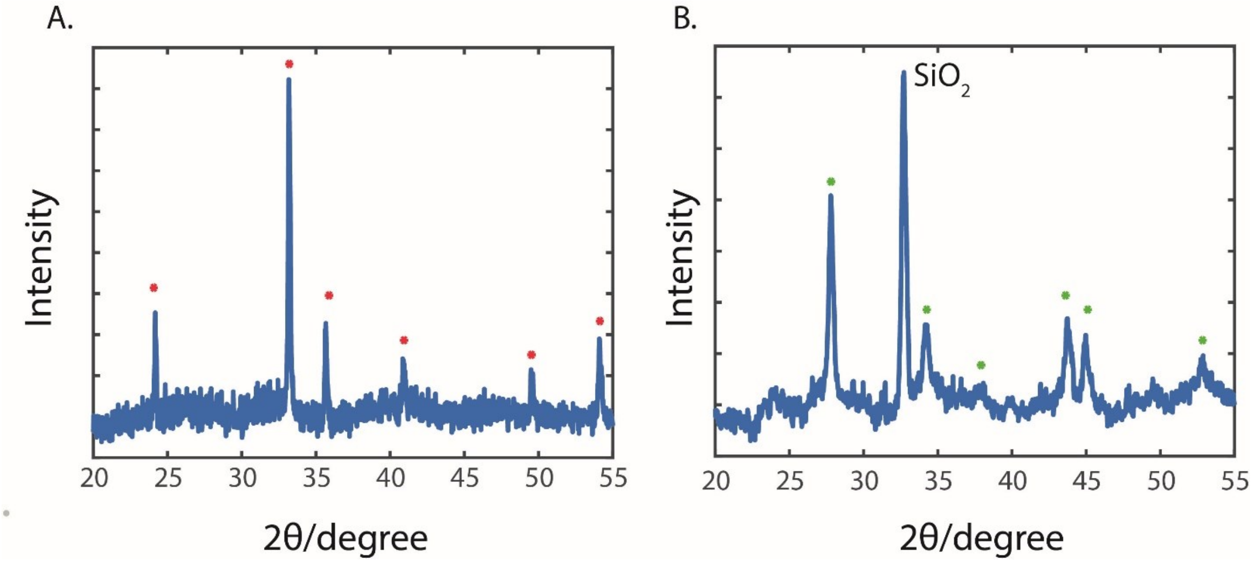

Figure S2. XRD of hematite(A) and akageneite(B). The red spots indicate the featured α-Fe_2O_3 peaks. The green spots indicate the featured β-FeOOH peaks.

S2.3 UV-Vis spectrum

The UV-Vis spectrum of hematite and akageneite indicates that the band gap of hematite is 2.1eV and the band gap of akageneite is 2.5eV.

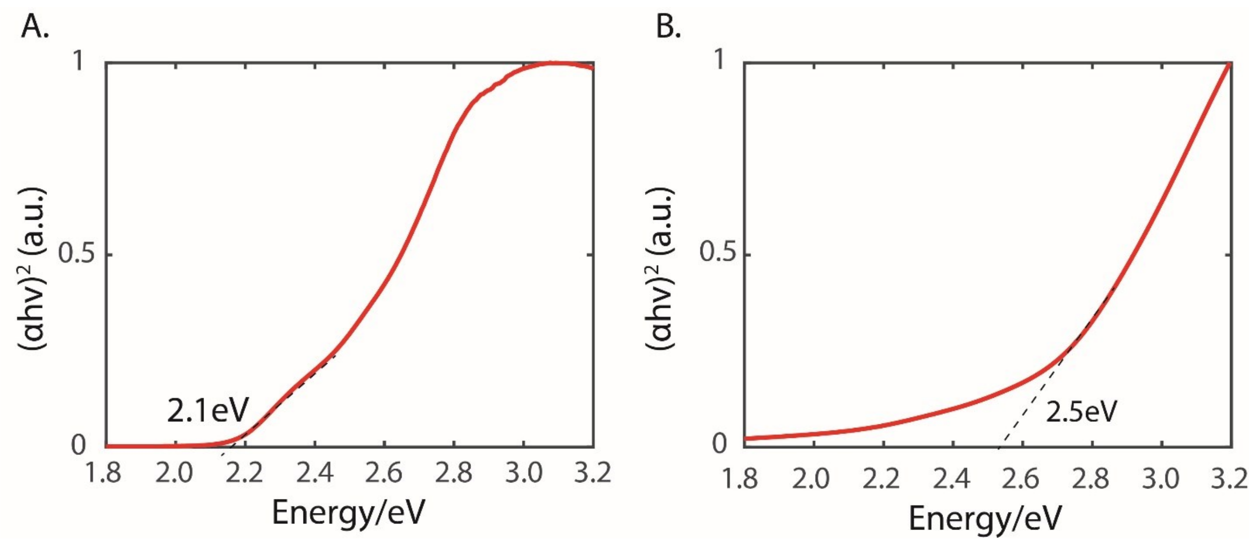

Figure S3. UV-Vis spectrum of hematite(A) and akageneite(B).

S3. Two-temperature model

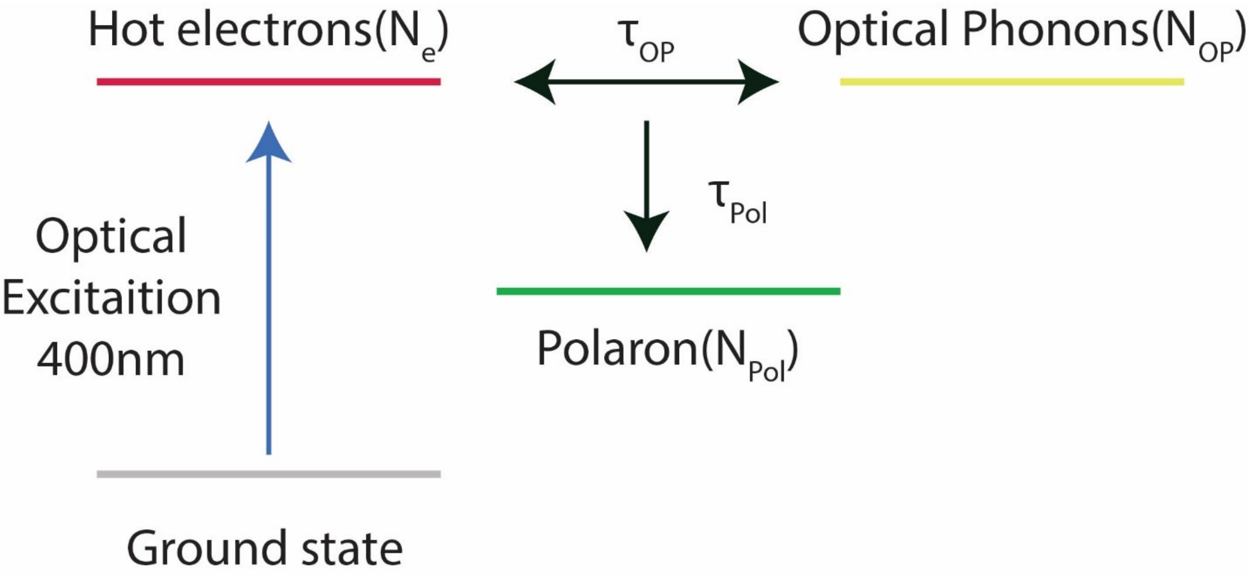

Figure S4. Schematic drawing of two temperature model of polaron formation. N_e is the population of hot electrons, N_{OP} is the population of optical phonon, N_{Pol} is the population of polaron. τ_{OP} is the electron-phonon scattering time constant, τ_{Pol} is the time constant of polaron formation.

The two-temperature model are illustrated in figure S4. Hot electrons(N_e) are generated after the photo excitation. Subsequently, hot electrons thermalized by scattering and excited optical phonons(N_{OP}). The hot electrons then combined with the optical phonons and generated polaron(N_{Pol}). The population follows the equations:

$$\frac{dN_e}{dt}=-\frac{N_e-N_{OP}}{\tau_{OP}}-\frac{N_e*N_{OP}}{\tau_{Pol}} \tag{1}$$

$$\frac{dN_{OP}}{dt}=\frac{N_e-N_{OP}}{\tau_{OP}}-\frac{N_e*N_{OP}}{\tau_{Pol}} \tag{2}$$

$$\frac{dN_{Pol}}{dt}=\frac{N_e*N_{OP}}{\tau_{Pol}} \tag{3}$$

The initial state time trace and the final state time trace are fitted to N_e and N_{Pol} with two weighting numbers. The time constant τ_{OP} are constrained at 30fs[1]. The time constant τ_{Pol} and the two weighting numbers are obtained by fitting the experimental data with the above equation.

S4. Static reflection simulation

The CTM4XAS software was used to simulate the stick spectrum of Fe^{3+} absorption coefficient. The crystal field splitting is 1.45eV and the Slater integral reduction is 50%. After obtaining the stick plot, we applied a Lorentzian broadening with a linear increase from 0.1eV at 51.5eV and 1.5eV at 55eV and a Fano asymmetric parameter of 3.5 to the stick plot[2]. Then, the refractive index was calculated by equation κ=λησ/4π, λ is the wavelength of light, η is the number density of the resonant absorber, σ is the absorption cross-section. The real part of refractive index can be calculated by kronig-kramers relation $n(\omega) = 1 + \frac{2}{\pi}P\int_0^\infty \frac{\omega'\kappa(\omega')}{\omega'^2 - \omega^2}d\omega'$, P refers to the Cauchy principle value of the integral, ω is the angular frequency of the light. As explained in the main text, we found that an offset on both real part and imaginary part of refractive index are necessary to fit the XUV spectra. The final complex refractive index $N(\omega)=n(\omega)+n_{offset}+i(\kappa(\omega)+\kappa_{offset})$. The reflectance $R = \left|\frac{-N^2cos(\theta) + \sqrt{N^2 - sin^2\theta}}{N^2cos(\theta) + \sqrt{N^2 - sin^2\theta}}\right|^2$, N is the complex refractive index, θ is the incident angle of probe beam at the sample plane. Figure S5 shows the simulated refractive index of hematite and akageneite. Figure S6 shows the dynamic of the offset of imaginary part of refractive index.

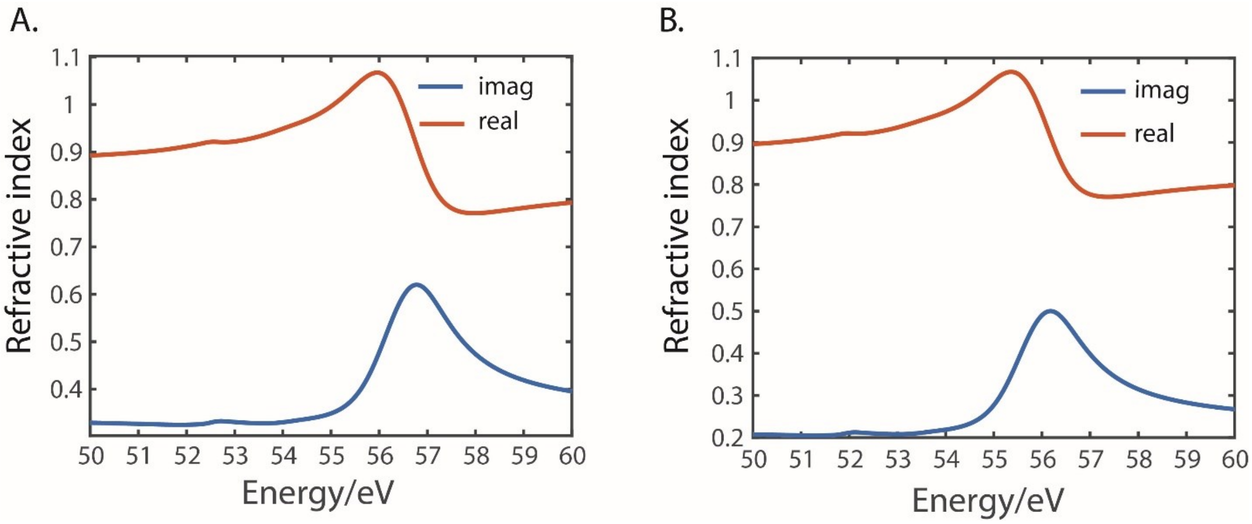

Figure S5 Real part and imaginary part of refractive index of hematite(A) and akageneite(B).

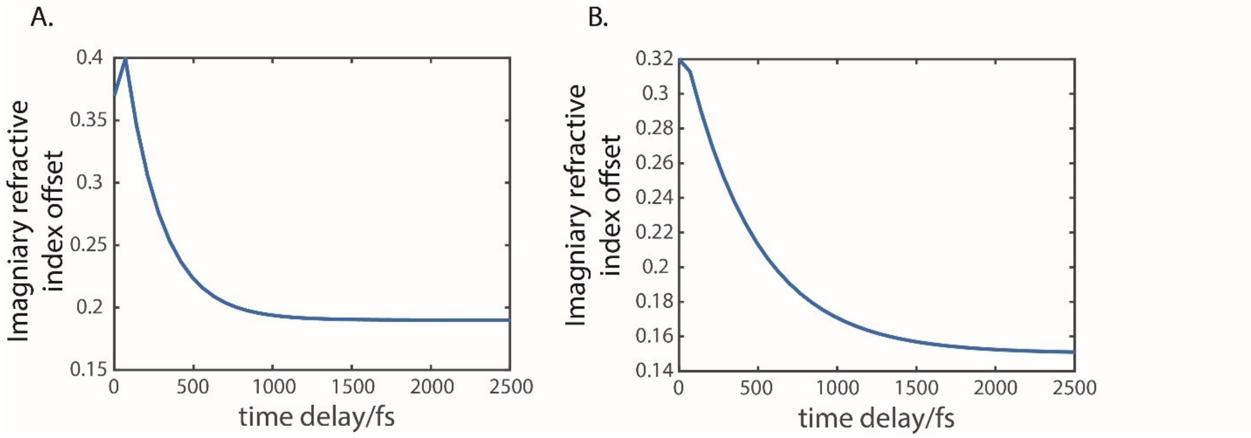

Figure S6. Time trace of imaginary refractive index offset of (A). hematite and (B). akageneite.

S5. Initial state spectra simulation

The initial state spectra can be simulated by calculating the reflectance of Fe^{2+}. Compared to Fe^{3+} reflection, the crystal field splitting of Fe^{2+} is 1.1eV, the slater integral reduction is 50%[3]. A Lorentzian broadening with a linear increase from 0.1eV at 51.5eV and 1.5eV at 55eV and a Fano asymmetric parameter of 3.5 are applied. Figure S7 shows the simulation result. The offset in imaginary part of refractive index for hematite is from 0.32 to 0.37, for akageneite is from 0.2 to 0.32. We noticed that the initial state simulation is not perfect. This could due to the non-thermalized distribution of hot electrons, causing the simulation only qualitatively match with the experimental result.

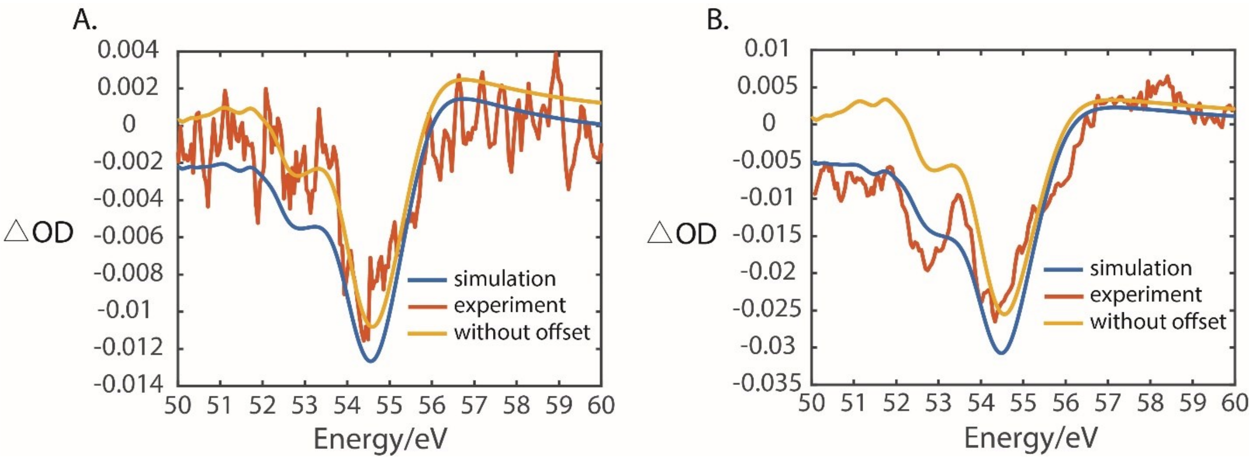

Figure S7. Comparison between the simulated and experimental transient initial state spectra of (A) hematite and (B) akageneite.

S6. Relaxation energy at different self-trapping energy

In the main text, we estimated that the self-trapping energy of akageneite is smaller than hematite. Based on this relation and $\Delta E_{act} = (-E_{exc} - E_{st} + E_{rel})^2/4E_{rel}$, we can compare the relaxation energy of akageneite to hematite. Figure S8 showed the relation between the relaxation energy of hematite and akageneite at different assumed self-trapping energy of akageneite. The result clearly showed that at different assumed self-trapping energy of akageneite, the relaxation energy of akageneite is always smaller than that of hematite. Previously literature has reported that the surface relaxation energy of hematite is 1.5eV. The calculated relaxation energy of akageneite is 1.2eV at 0.22eV self-trapping energy, 1.25eV at 0.27eV self-trapping energy, 1.3eV at 0.32eV self-trapping energy of akageneite.

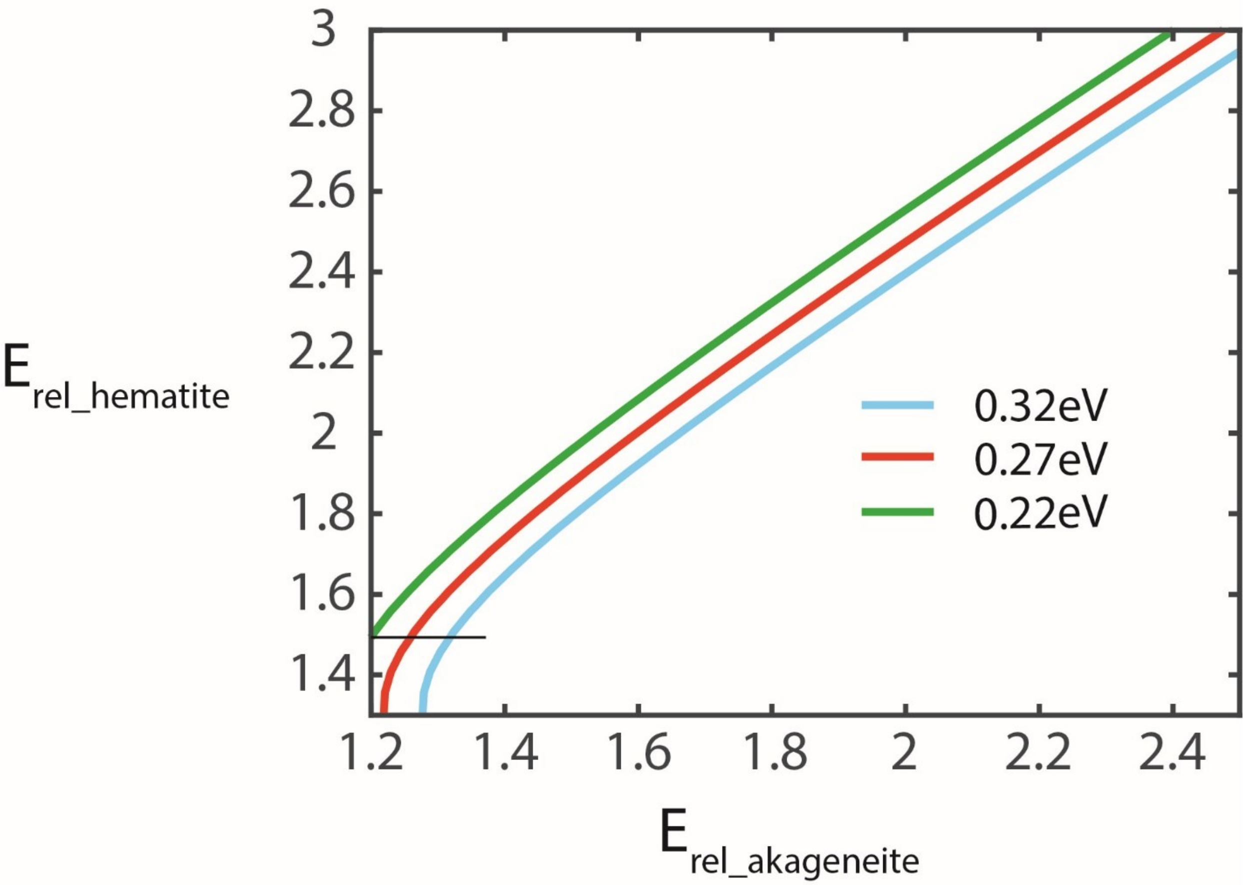

Figure S8. The relation between the relaxation energy of hematite and akageneite at different assumed self-trapping of akageneite.

Reference

1 S. Biswas, S. Wallentine, S. Bandaranayake and L. R. Baker, *J. Chem. Phys.*, 2019, **151**, 104701.

2 L. M. Carneiro, S. K. Cushing, C. Liu, Y. Su, P. Yang, A. P. Alivisatos and S. R. Leone, *Nat. Mater.*,

2017, **16**, 819–825.

3 A. Cirri, J. Husek, S. Biswas and L. R. Baker, *J. Phys. Chem. C*, 2017, **121**, 15861–15869.